1-1-2016

Fluoroscopic System for Assessment of *In Vivo* Hindfoot Kinematics During Gait: Control Data and Applications in Osteogenesis Imperfecta

Ben McHenry
Marquette University, ben.mchenry@marquette.edu

Jason Long
cincinnati Children's Hospital Medical Center, Cincinnati, OH

Peter Smith
Shriners Hospitals for Children, Chicago, IL

Haluk Altiok
Shriners Hospitals for Children

Gerald F. Harris
Marquette University, gerald.harris@marquette.edu

Published version. *Transitional Care in Osteogenesis Imperfecta: Advances in biology, Technology, and Clinical Practice*, (2016): pp. 285-300. Publisher link.

17 FLUOROSCOPIC SYSTEM FOR ASSESSMENT OF *IN VIVO* HINDFOOT KINEMATICS DURING GAIT: CONTROL DATA AND APPLICATIONS IN OSTEOGENESIS IMPERFECTA

Benjamin McHenry, Ph.D.[1]
Jason Long, Ph.D.[2]
Peter Smith, M.D.[3]
Haluk Altiok, M.D.[3]
Gerald Harris, Ph.D., P.E.[1,3]

[1] Orthopaedic and Rehabilitation Engineering Center (OREC),
Marquette University and The Medical College of Wisconsin, Milwaukee, WI
[2] Cincinnati Children's Hospital Medical Center, Cincinnati, OH
[3] Shriners Hospitals for Children, Chicago, IL

INTRODUCTION

Literature suggests that the children with type I osteogenesis imperfecta (OI) suffer from a variety of abnormal gait characteristics which include a reduction in power generation during push off.[1,2] This reduction is of interest clinically because 80% of the power associated with normal ambulation is derived from push off, and is often the gold standard used in defining a normal gait pattern. The exact biomechanical reasons for this reduction in push off power seen in patients with type I OI are not well understood, but a fluoroscopic *in vivo* assessment of the foot may reveal some clues.

Historically, *in vivo* lower extremity modeling has been accomplished by defining a system of segments in which the most distal segment is a rigid representation of the entire foot.[3-7] This rigid representation of the foot fails to account for the known articulations within the foot, and can lead to errors in gait analysis, especially when applied to the deformed foot.[8,9] To overcome the shortcomings of defining the foot as a single rigid segment, several multi-

segmental foot models are described in the literature. These models use externally placed markers on the skin to break the foot into multiple segments, ranging from as few as two to as many as nine segments.[10-16] While these multi-segmental foot models provide a more accurate representation of the motion of the deformed foot, they have shortcomings associated with external marker use and rigid segment assumptions.

Any human locomotion model using external markers attached to the skin to track underlying bone has potential error associated with soft tissue artifacts (STA). These artifacts arise because superficial muscle and skin are free to move relative to the underlying bony anatomy, making it difficult to reliably measure the bony movement of interest. A recent hindfoot study using single-plane fluoroscopy reported translational soft tissue artifact at the calcaneus ranging from 5.9 ± 7.3 mm at heel strike to 12.1 ± 0.3 mm at toe off.[17] Several additional studies have attempted to quantify and reduce this source of error, but none have demonstrated a reliable way to do it.[18-21] In general, STA are: (1) dependent on the anatomic location of interest, (2) dependent on the task being measured, (3) different between subjects, and (4) of a frequency content similar to the movement of interest, such that they cannot be filtered out.[22]

In addition to STA, marker placement repeatability errors arise in current multi-segmental foot models and can be directly attributed to the use of external markers. Marker locations are usually used in conjunction with anthropomorphic data to mathematically determine anatomic locations or to define local coordinate systems. Because of this, external marker placement becomes critical in the evaluation of the model. Most models use easily palpable landmarks as locations to place external markers, though a number of studies have quantified errors associated with finding them. Della Croce et al. measured the precision with which lower limb anatomic locations could be repeatedly determined and reported values at the foot as high as 10.3mm and 21.5 mm for intra and inter-examiner precision respectively.[23] A similar study done by Rabuffetti et al. reported inter-examiner precision values at the lateral malleolus and fifth metatarsal head of 9.2 mm and 7.0 mm respectively.[24] These misplacement errors propagate through the kinematic model and end up affecting the reported results. Della Croce et al. estimated intra- and inter-examiner precision of ankle joint angles during upright posture as high as 3.9° and 10.9° respectively.[23]

The reliability of marker placement has a direct effect on joint kinematics. In joints that undergo small ranges of motion (such as those intra-foot), the error associated with marker misplacement can be considerable.[25] As the distance between external markers decreases (e.g., when defining multiple segments in the small volume occupied by the foot), error associated with marker placement repeatability can increase, resulting in angle definition sensitivity.[26]

In addition to the errors associated with STA and marker placement, multi-segmental foot models make rigid body assumptions in segments containing multiple bones. The validity of these rigid body assumptions (i.e., the question of whether the bones within the segment move with respect to each other) directly affects the kinematic data resulting from these segments. There is a risk of attributing motion to a joint where it is not actually taking place, or of missing a motion entirely. Nester et al. reported specifically on the error associated with rigid body violations of mid and forefoot segments and concluded that there was clear evidence of how different bone groupings influenced a segment's kinematics.[27] The only way to correct for this is to subdivide the segment into more segments; for a marker-based model, this requires the use of more markers, which may be affixed either externally or internally (i.e. by invasive means). Internally fixed bone-anchored markers, for example, are often regarded as a solution to the rigid body assumption. However, because of their invasive nature and potential for altering gait, they are rarely used for clinical assessment.

To address these limitations, the aim of this study was to develop a multi-segmental hindfoot model that used fluoroscopy to define bony segment position. The planar fluoroscopic images obtained from the described system were used to determine talocrural and subtalar kinematics in the sagittal plane. These kinematics compare favorably to those reported by more invasive means.

METHODS

Participants

The right feet of five subjects were tested after institutional review approval and informed consent (5 Male; 22.8 ± 4.0 years of age). All subjects demonstrated normal lower extremity function and had no prior lower extremity injuries.

Protocol

Each subject underwent standard barefoot gait analysis with simultaneous fluoroscopic image collection at 120Hz. Following dynamic data collection, subjects were escorted to a nearby x-ray suite where a single limb support barefoot x-ray was taken of their right foot placed at the same foot progression angle observed during dynamic image collection. The developed multi-segmental hindfoot model was then applied to the collected data.

Gait Analysis

Motion data was collected at 120Hz using a 14 camera motion capture system (Vicon Motion Systems, Inc., Lake Forest, CA) while subjects walked across a raised six meter long walkway. Reflective markers were placed at specific anatomic landmarks and were used to define a tibial coordinate system, foot progression angle, and global referencing points for each of the collected fluoroscopic images (Table 1). Subjects were asked to walk at a self-selected pace for a maximum of five trials of fluoroscopic exposure.

Table 1. External marker locations. Markers M1 and M2 are used to define the foot progression angle (β) in Equation 2. Markers M3-M6 are used to define the axes of the tibial coordinate system.

Marker Name	Marker Location
M1	Calcaneal tuberosity
M2	Head of the 2nd metatarsal
M3	Medial malleolus
M4	Lateral malleolus
M5	Medial femoral epicondyle
M6	Lateral femoral epicondyle

Fluoroscopic Imaging

Fluoroscopic images were collected at 120 fps using a Basler Aviator avA1000km camera (Basler Vision Technologies, Ahrensburg, Germany), XCAP imaging software (XCAPTM, Buffalo Grove, IL), and a reconfigured OEC 9000 C-arm fluoroscopy unit (GE, Fairfield, CT). Ground reaction force data was collected using a multi-axis AMTI OR6-5-1 force plate (AMTI, Watertown, MA) embedded in a raised walkway. Figure 1 illustrates the system configuration. The image intensifier was placed flush with the force plate (global XZ plane) and slightly below the raised walkway to allow the best view of the stance phase of gait. Because both the gait analysis motion data and fluoroscopic images were collected at 120Hz, the fluoroscopic

images could be synchronized to the motion data (during data processing) by use of the ground reaction force and a five-volt TTL pulse (emitted by the fluoroscopy unit when activated). In addition to synchronization, the fluoroscopic images underwent a linearization process to correct for the pincushion image distortion created by the tube nature of the image intensifier.[28]

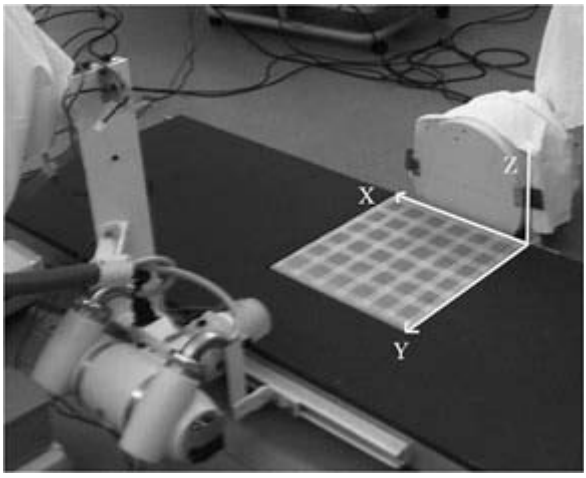

Figure 1. System configuration: Embedded force plate with global coordinate system, emitter (nearside), and image intensifier (far side).

Static X-Ray

After gait analysis motion data was collected, the average foot flat progression angle was calculated for all trials by using external markers. This average progression angle was used to position the foot for a lateral, single limb support x-ray. The foot was positioned for the x-ray such that it matched the position of foot flat during the walking trials.

Hindfoot Model

A three-segment rigid body model was developed to describe the kinematics of the hindfoot during the stance phase of gait. The segments were: (1) tibia, (2) talus, and (3) calcaneus. The tibial segment coordinate system was defined completely by external markers as it remained outside the image intensifier field of view for much of stance. The talar and calcaneal segment coordinate systems were defined by first locating virtual markers in the fluoroscopic images (i.e. image coordinates) and translating them into global coordinates by a method of global referencing. Because only one fluoroscopic

unit was used in this study virtual markers were translated into a 2D motion plane. The motion plane was the foot progression plane; or the plane that includes the M1 and M2 markers and is perpendicular to the global XY plane (see Figure 2). Translating virtual marker points of interest from image coordinates (POIx', POIz') to global coordinates (POIX, POIY, POIZ) within the motion plane required having a reference point and knowledge about the magnification of the foot in the images. The reference point must have coordinates that are known in both the image and global coordinate systems and must also be contained within the motion plane. For the fluoroscopic images, marker M1 is used as the reference point because it is contained by the motion plane and has known image and global coordinates ((Hx', Hz') and (HX, HY, HZ) respectively). The magnification of the foot in the fluoroscopic images is determined by adhering two radiographic markers to the subject's ankle 30mm from each other. The pixel distance between these markers is then determined in the fluoroscopic images and a constant pixels per millimeter (ppm) variable is calculated. Equations 1-3 (Table 2) are used to translate points of interest from image coordinates to global coordinates within the motion plane. Figure 3 shows a typical fluoroscopic image where several parameters in equations 1-3 are defined (note: only parameters θ and ppm are constants for each trial, all other parameters are calculated for each fluoroscopic image).

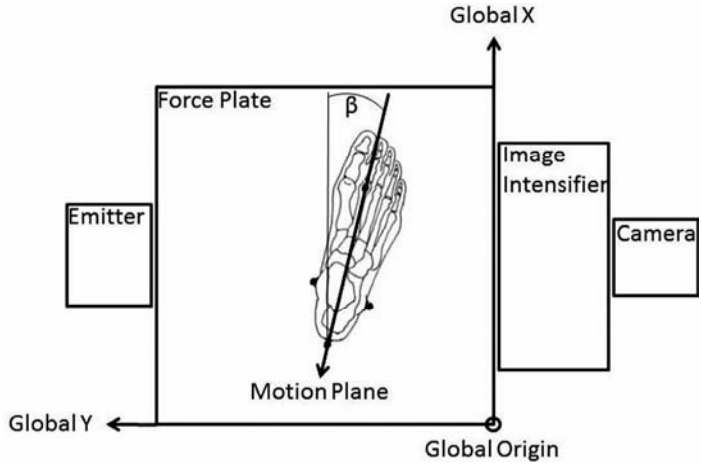

Figure 2. Motion plane. The plane of motion is perpendicular to global XY plane through markers on the calcaneal tuberosity and the superior head of the second metatarsal.

Table 2. Global referencing equations.

$$POIX = HX + \left[\left[\frac{POIx' - Hx'}{ppm}\right]\cos\theta + \left[\frac{POIz' - Hz'}{ppm}\right]\sin\theta\right] \quad \text{(Eq. 1)}$$

$$POIY = HY + \left[\left[\frac{POIx' - Hx'}{ppm}\right]\cos\theta + \left[\frac{POIz' - Hz'}{ppm}\right]\sin\theta\right]\tan\beta \quad \text{(Eq. 2)}$$

$$POIZ = HZ + \left[-\left[\frac{POIx' - Hx'}{ppm}\right]\sin\theta + \left[\frac{POIz' - Hz'}{ppm}\right]\cos\theta\right] \quad \text{(Eq. 3)}$$

Figure 3. Typical fluoroscopic image. POI locations are translated from image coordinates (POIx', POIz') to global (POIX, POIY, POIZ) using an external marker's image (Hx', Hz') and global (HX, HY, HZ) coordinate locations, as well as the image pixels per millimeter (ppm) magnification, subject foot progression angle (β, calculated from external markers), and the camera's angular rotation from global (θ).

Two virtual markers for the talus (V1, V2) as well as two for the calcaneus (V3, V4) (Figure 4) were globally referenced (Table 2) for each of the fluoroscopic images. These virtual marker locations were subject specific and were chosen because they were easily identified in all fluoroscopic

images. After virtual marker locations were translated to global coordinates via global referencing, they were used in conjunction with external skin marker locations to define the local coordinate axes of the tibial, talar and calcaneal coordinate systems (Table 3).

Once coordinate systems were defined for all three segments the anatomical joint angles for the talocrural and subtalar joint were determined using the Joint Coordinate Method.[29] as described by Vaughn et al.[30] After the anatomical joint angles were determined, they were compared to the angles of quiet standing (quiet standing angles were determined by applying the developed model to the static x-ray image for each subject). The measured angles during quiet standing are used for clinical reference and represent neutral position for reported kinematics.

Figures 4. Virtual marker locations. V1 and V2 represent typical virtual marker locations for the talus, while V3 and V4 represent typical virtual marker locations for the calcaneus.

Table 3. Segment coordinate system axes definition. Virtual markers have prefix V, external markers have prefix M. All marker locations (virtual and external) are defined in global coordinates.

Segment	i-axis	j-axis	k-axis
Calcaneus	$\frac{(V3-V4)}{\lvert(V3-V4)\rvert}$	$\frac{(k_{axis}\times i_{axis})}{\lvert(k_{axis}\times i_{axis})\rvert}$	$\frac{(i_{axis}\times(0,0,1))}{\lvert(i_{axis}\times(0,0,1))\rvert}$
Talus	$\frac{(V1-V2)}{\lvert(V1-V2)\rvert}$	$\frac{(k_{axis}\times i_{axis})}{\lvert(k_{axis}\times i_{axis})\rvert}$	$\frac{(i_{axis}\times(0,0,1))}{\lvert(i_{axis}\times(0,0,1))\rvert}$
Tibia	$\frac{\left(\frac{M5+M6}{2}\right)-\left(\frac{M3+M4}{2}\right)}{\left\lvert\left(\left(\frac{M5+M6}{2}\right)-\left(\frac{M3+M4}{2}\right)\right)\right\rvert}$	$\frac{\left(\left(M3-\left(\frac{M3+M4}{2}\right)\right)\times i_{axis}\right)}{\left\lvert\left(\left(M3-\left(\frac{M3+M4}{2}\right)\right)\times i_{axis}\right)\right\rvert}$	$\frac{(i_{axis}\times j_{axis})}{\lvert(i_{axis}\times j_{axis})\rvert}$

RESULTS

Figure 5 shows the talocrural and subtalar sagittal plane kinematics for a single subject and demonstrates the repeatability of the model to measure hindfoot kinematics trial to trial. Figure 6 shows the talocrural and subtalar kinematics for all five subjects combined. The X axis on Figures 5 and 6 represents the % Stance Phase of gait, with 0% representing heel strike and 100% representing toe off. Because the calcaneus and talus are no longer in the fluoroscopic field of view at toe off, most trials do not have data through 100% of the gait cycle, which manifests with missing data towards the end of Stance Phase. Table 4 shows the mean peak plantar and dorsiflexion values for the talocrural and subtalar kinematics, respectively, for all five subjects combined.

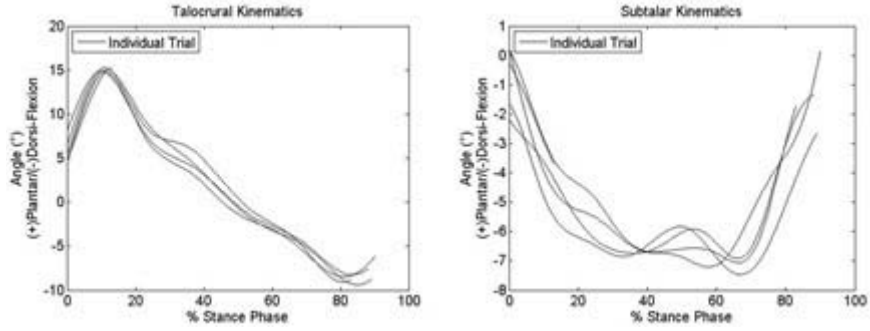

Figure 5. Sagittal plane kinematic results. Black lines represent individual trials for a single subject.

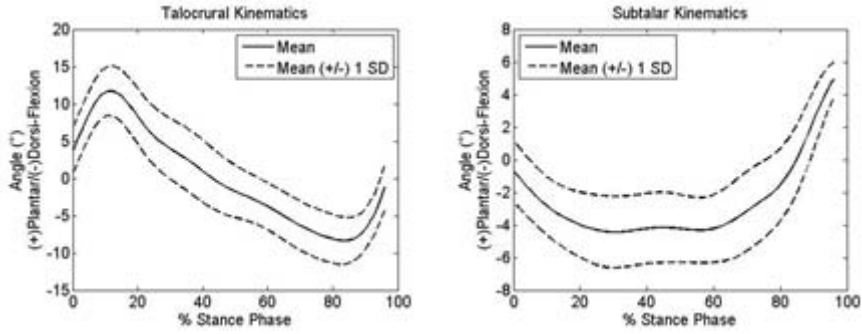

Figure 6. Sagittal plane kinematic results. Solid line represents mean angle of all five subjects combined. Dashed lines represent mean ± 1 SD.

Table 4. Kinematic statistics.

TALOCRURAL JOINT MOTION		
Peak Plantar Flexion	11.70°	@ 12% of Stance Phase
Peak Dorsiflexion	8.36°	@ 83% of Stance Phase
Range	20.06°	
SUBTALAR JOINT MOTION		
Peak Plantar Flexion	5.45°	@ 96% of Stance Phase
Peak Dorsiflexion	4.44°	@ 30% of Stance Phase
Range	9.89°	

DISCUSSION

Talocrural joint motion starts in a neutral position and slopes towards plantar flexion during heel strike, reaching peak plantar flexion around 12% of stance (Figure 6). After foot flat occurs, the tibia rolls over the talus forcing the talocrural joint into dorsiflexion which lasts until about 83% of stance. As push off occurs, the talocrural joint once again moves towards plantar flexion. Talocrural range of motion (ROM) for the five subjects combined is 20.06° (Table 4). As shown in Figure 6, subtalar motion is primarily in dorsiflexion during stance phase, moving into plantar flexion around 84% of stance. Subtalar ROM for the five subjects combined is 9.89° as reported in Table 4.

Other than the fluoroscopic method described in the current study, only bone anchored marker studies report both talocrural and subtalar motion during the entire stance phase of gait. These studies rely on intra-cortical pins to be surgically inserted into the various bones of the foot/ankle. Attached to the

ends of these pins is a cluster of markers whose motion is captured using stereophotogrammetry. The advantages of using bone pins is that STA is no longer present, and bones with few palpable landmarks can be tracked directly (not combined with other bones). A study by Arndt et al. tested three subjects using surgically inserted intra-cortical pins and reported both talocrural and subtalar motion.[31,32] The results of the Arndt study compared to the fluoroscopic talocrural and subtalar results are shown in figures 7 and 8 respectively.

As shown in figure 7, the shape and pattern of talocrural joint motion in both studies is quite similar. Peak plantar flexion for both studies occurs between 10-15% of gait, and peak dorsiflexion occurs between 80-85%. Figure 8 shows similar results in subtalar motion between the studies, with peak plantar flexion occurring between 20-30% of stance, and peak dorsiflexion occurring between 95-100%. The major differences in the kinematics of the two studies is seen in overall ROM, with the fluoroscopic study subjects combined averaging 20.1° and 9.9° for talocrural and subtalar motion respectively, and the Arndt study subjects combined averaging 11.7° and 2.8° respectively.[31,32] Reasons for the reduced ROM seen in the Arndt study compared to the fluoroscopic study may be attributed to methodological differences between studies. The Arndt study uses intra-cortical pins to avoid STA and muti-bone segment rigidity assumptions. While the intra-cortical pins are effective in these areas, their use is considered invasive and studies need to be undertaken to quantitatively ensure they do not alter normal gait function. The fluoroscopic study is 2D in nature and is dependent on the clinician to locate the virtual markers in every collected fluoroscopic frame. While requiring the clinician to locate virtual markers in every frame is a good way of self-correcting marker location frame to frame, any out of plane motion which appears to alter in-plane marker placement will not be noticed by the clinician, and out of plane motion could be falsely reported as occurring in plane. In addition, the fluoroscopic study group consisted of younger individuals (22.8 years) than the bone pin kinematic studies (39.3 years).[31,32] Oberg et al. has described differences in gait kinematics with aging for 233 healthy subjects aged 10-79 years.[33] While these differences are small, the effects of age upon *in vivo* bony kinematics of the foot and ankle have not been studied.

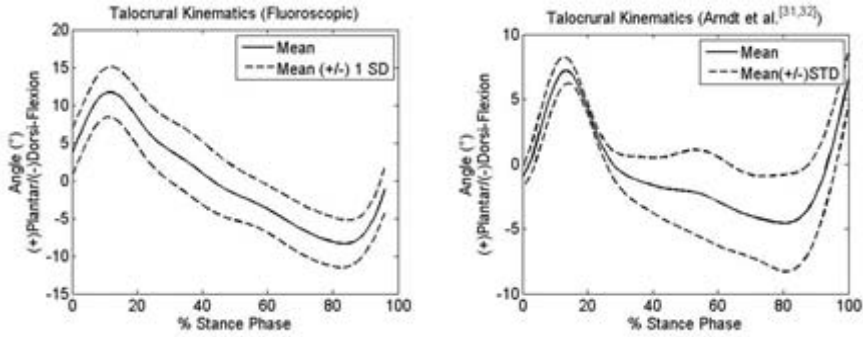

Figure 7. Sagittal plane talocrural kinematics. Solid line represents mean angle of all subjects combined. Dashed lines represent mean ± 1 SD. The fluoroscopic study consisted of 5 subjects, while the Arndt et al. study consisted of 3 subjects.[31,32]

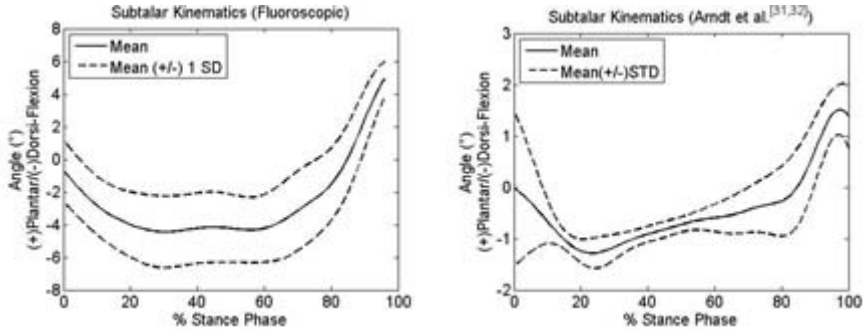

Figure 8. Sagittal plane subtalar kinematics. Solid line represents mean angle of all subjects combined. Dashed lines represent mean ± 1 SD. The fluoroscopic study consisted of 5 subjects, while the Arndt et al. study consisted of 3 subjects.[31,32]

CONCLUSION

The use of fluoroscopy shows promise in the foot and ankle motion analysis. Unlike current multi-segment foot models, fluoroscopic models do not suffer from assumptions made about STA, marker placement repeatability, or segment rigidity, and are completely non-invasive. In addition to the mentioned advantages, the radiographic nature of fluoroscopy would allow for the described model to be easily applied to the shod foot (which would be nearly impossible using external or bone anchored markers) and since most of human ambulation occurs in the shod condition, knowledge of how the bones of the foot and ankle move within a shoe would be of great clinical significance.

Study limitations include a narrow sample of adult male subjects aged 18 to 28 with no reported gait deficiencies or prior bony foot injury. The current study is also limited to a single plane (sagittal) analysis of hindfoot motion components. A further limitation is the use of ionizing radiation with current levels estimated at 10 μSv/trial. According to the USNRC, whole body annual occupational limits are 5 rems (50,000 μSv).

ACKNOWLEDGEMENTS

The contents of this study were developed under a grant from the Department of Education, NIDRR grant number H133E100007. However, the contents do not necessarily represent the policy of the Department of Education, and you should not assume endorsement by the Federal Government. This study was additionally supported by Shriners Hospitals for Children, and the Pedorthic Foundation.

REFERENCES

1. Graf, A., et al., Gait characteristics and functional assessment of children with type I osteogenesis imperfecta. *J Orthop Res* 2009;27(9):1182-90.
2. Krzak, J.J., et al., Analysis of Push-Off Power During Locomotion in Children with Type 1 Osteogenesis Imperfecta. *Journal of Experimental and Clinical Medicine* 2011;3(5):195-199.
3. Apkarian, J., S. Naumann, and B. Cairns, A three-dimensional kinematic and dynamic model of the lower limb. *J Biomech* 1989;22(2):143-55.
4. Cappozzo, A., T. Leo, and A. Pedotti, A general computing method for the analysis of human locomotion. *J Biomech* 1975;8(5):307-20.
5. Kadaba, M.P., H.K. Ramakrishnan, and M.E. Wootten, Measurement of lower extremity kinematics during level walking. *J Orthop Res* 1990;8(3):383-92.
6. Ounpuu, S., J.R. Gage, and R.B. Davis, Three-dimensional lower extremity joint kinetics in normal pediatric gait. *J Pediatr Orthop* 1991;11(3):341-9.
7. White, S.C., H.J. Yack, and D.A. Winter, A three-dimensional musculoskeletal model for gait analysis. Anatomical variability estimates. *J Biomech* 1989;22(8-9):885-93.
8. Davis, R.B., et al., The Design, Development, and Initial Evaluation of a Multisegment Foot Model for Routine Clinical Gait Analysis, in *Foot and Ankle Motion Analysis: Clinical Treatment and Technology*, G.F. Harris, P.A. Smith, and R.M. Marks, Editors. 2008, CRC Press. p. 425-444.
9. Harris, G.F., Analysis of Ankle and Subtalar Motion During Human Locomotion, in *Inman's Joints of the Ankle*, J.B. Stiehl, Editor. 1991, Williams & Wilkins. p. 75-84.
10. Hunt, A.E., et al., Inter-segment foot motion and ground reaction forces over the stance phase of walking. *Clin Biomech* 2001;16(7):592-600.
11. Hwang, S.J., H.S. Choi, and Y.H. Kim, Motion analysis based on a multi-segment foot model in normal walking. *Conf Proc IEEE Eng Med Biol Soc* 2004;7:5104-6.

12. Jenkyn, T.R. and A.C. Nicol, A multi-segment kinematic model of the foot with a novel definition of forefoot motion for use in clinical gait analysis during walking. *J Biomech* 2007;40(14):3271-8.
13. Kidder, S.M., et al., A system for the analysis of foot and ankle kinematics during gait. *IEEE Trans Rehabil Eng* 1996;4(1):25-32.
14. Leardini, A., et al., Rear-foot, mid-foot and fore-foot motion during the stance phase of gait. *Gait Posture* 2007;25(3):453-62.
15. Leardini, A., et al., An anatomically based protocol for the description of foot segment kinematics during gait. *Clin Biomech* 1999;14(8):528-36.
16. MacWilliams, B.A., M. Cowley, and D.E. Nicholson, Foot kinematics and kinetics during adolescent gait. *Gait Posture* 2003;17(3):214-24.
17. Shultz, R., A.E. Kedgley, and T.R. Jenkyn, Quantifying skin motion artifact error of the hindfoot and forefoot marker clusters with the optical tracking of a multi-segment foot model using single-plane fluoroscopy. *Gait Posture* 2011;34(1):44-8.
18. Okita, N., et al., An objective evaluation of a segmented foot model. *Gait and Posture* 2009;30(1):27-34.
19. Shultz, R., A.E. Kedgley, and T.R. Jenkyn, Quantifying skin motion artifact error of the hindfoot and forefoot marker clusters with the optical tracking of a multi-segment foot model using single-plane fluoroscopy. *Gait and Posture* 2011;34(1):44-48.
20. Tranberg, R. and D. Karlsson, The relative skin movement of the foot: a 2-D roentgen photogrammetry study. *Clin Biomechs* 1998;13(1):71-76.
21. Wrbaskic, N. and J.J. Dowling, An investigation into the deformable characteristics of the human foot using fluoroscopic imaging. *Clin Biomech* 2007;22(2):230-238.
22. Leardini, A., et al., Human movement analysis using stereophotogrammetry: Part 3. Soft tissue artifact assessment and compensation. *Gait and Posture* 2005;21(2):212-225.
23. della Croce, U., A. Cappozzo, and D.C. Kerrigan, Pelvis and lower limb anatomical landmark calibration precision and its propagation to bone geometry and joint angles. *Med Biol Eng Comput* 1999;37(2):155-61.
24. Rabuffetti, M., et al., Self-marking of anatomical landmarks for on-orbit experimental motion analysis compared to expert direct-marking. *Human Movement Science* 2002;21(4):439-455.
25. Della Croce, U., et al., Human movement analysis using stereophotogrammetry: Part 4: assessment of anatomical landmark misplacement and its effects on joint kinematics. *Gait and Posture* 2005;21(2):226-237.
26. Della Croce, U., et al., Human movement analysis using stereophotogrammetry: Part 4: assessment of anatomical landmark misplacement and its effects on joint kinematics. *Gait and Posture* 2005;21(2):226-237.
27. Nester, C., et al., Error in the description of foot kinematics due to violation of rigid body assumptions. *Journal of Biomechanics* 2010;43(4):666-672.
28. Karau, K.L., et al., Microfocal X-ray CT imaging and pulmonary arterial distensibility in excised rat lungs. *Am J Physiol Heart Circ Physiol* 2001;281(3):H1447-57.
29. Grood, E.S. and W.J. Suntay, A joint coordinate system for the clinical description of three-dimensional motions: application to the knee. *Journal of Biomechanical Engineering* 1983;105(2):136.
30. Vaughan, C.L., B.L. Davis, and J.C. O'Connor, Dynamics of human gait. Vol. 2. 1992: Human Kinetics.

31. Arndt, A., et al., Ankle and subtalar kinematics measured with intracortical pins during the stance phase of walking. *Foot Ankle Int* 2004;25(5):357-64.
32. Arndt, A., Personal Communication 2012.
33. Oberg, T., A. Karsznia, and K. Oberg, Joint angle parameters in gait: reference data for normal subjects, 10-79 years of age. *J Rehabil Res Dev* 1994;31(3):199-213.